Journal of The Korean Nuclear Society
Volume 15, Number 2, June, 1983

《**Technical Report**》

Mechanisms, Experimental Results, Empirical Correlations and Analytic Models of Heat Transfer in Containment Building Following a LOCA

Jong Ho Choi and Soon Heung Chang

Korea Advanced Institute of Science and Technology

(Recieved March 23, 1983)

냉각재 상실 사고시 격납 용기내에 있어서의 열전달에 관한 기구, 실험결과, 선험 관계식 및 해석적 모형들에 관한 고찰

최 종 호·장 순 흥

한국과학기술원

(1983. 3. 23 접수)

Abstract

Estimates of the rate of heat removal from the containment atmosphere following a loss of colant accident (LOCA) are important to the prediction of containment peak pressure and temperature which are essential parameters in designing the containment building. An overall survey and discussion of mechanisms, experimental results, empirical correlations and analytical models that are relevant to the heat transfer inside the containment have been made. As a result of this review, the current state of the konwledge about the containment heat transfer can be understood and it is known that more investigations are needed to avoid the misuse of various correlations.

요 약

냉각재 상실 사고시에 격납 용기로부터 열 제거능력의 추정은 격납용기의 기본적인 설계변수인 최고 압력 및 온도의 예측에 있어서 매우 중요하다. 지금까지 격납 용기내의 열전달에 관하여 실험 및 해석적인 방법에 의해서 연구한 결과들을 종합하여 검토해 봄으로서 현재의 수준을 알 수 있었으며, 이들 관계식의 잘못된 사용을 피하고 보다 정확한 예측을 위해서는 더욱 깊은 연구가 필요하다고 생각된다.

I. Introduction

The containment systems of large nuclear power plants are designed to withstand the pressure and temperature that could result from a loss of coolant accident. The pressure reducing effects of steam condensation on the pressure-temperature response in a containment to a LOCA is a subject of safety concern both from the views of containment integrity and the performance capability of the emergency core

cooling systems (ECCS). The containment atmosphere, in the case of a LOCA, is pressurized by the release of high energy coolant into the containment atmosphere, and this pressure rise imposes a potential threat to the structural integrity of the containment building which is the final barrier against the release of radioactive material to the environments. The peak containment pressure is highly dependent on the heat transfer coefficient between the containment atmosphere and heat absorbing structures. Thus, heat transfer is related to design limits, construction cost, and margin of safety considerations. After the blowdown of the primary coolant, when the ECCS is activated for the core recovery, the cooling effectiveness by reflooding is reduced if a lower containment pressure is encountered. Although it may be conservative to have a higher containment pressure for the structural evaluation, it is less conservative to have the same pressure for analyzing the ECCS. The review of heat transfer coefficients divided into three different parts: experimental values, empirical correlations and analytical correlations based on analytical models.

2. Mechanisms involved in the heat transfer process

Heat is transferred from the hot atmosphere to the containment building structures and heat sinks by two important mechanisms: single phase convection and condensation. Radiation is not important because the existing temperature differences in the containment are relatively low. Conduction is only important inside the structures or heat sinks. The contribution due to condensation is usually larger than the one due to single phase convection. Condensation involves a phase change from vapor to liquid with high enthalpy changes.

Two separate time periods are generally considered following a LOCA in which different correlations for condensing steam heat transfer coefficients apply.[1] The first period is called the *blowdown period* characterized by high turbulence in the atmosphere as the primary coolant system decompresses. Forced convection, together with condensation of steam on the cold walls, are the major mechanisms for heat transfer during this period. The end point of this period is usually not defined explicitly but is the end of the pressurization of the containment resulting from the initial injection of primary coolant into the containment. The second period is referred to as the *post-blowdown period,* where natural convection and condensation are the main heat transfer mechanisms.

2.1. Convective heat transfer

Convective heat transfer is the process of energy transfer by both conduction and fluid motion. Steam and air move into the cooler boundary layer near the heat sink, give up part of their heat and are swept out again by convective currents. The rate of convective heat transfer is proportional to the total temperature

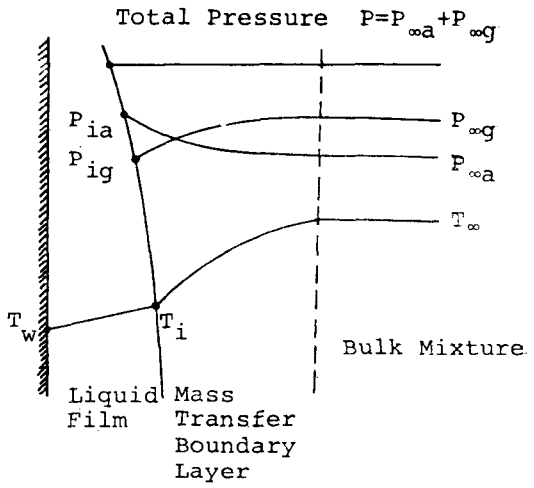

Fig. 1. Physical Picture of Condensing Surface

driving force $(T_\infty - T_w)$, and it increases with an increase in the convective driving force which is proportional to $(\rho_w - \rho_\infty)g$.

The value of the heat transfer coefficient can be calculated using analytical solutions or empirical correlations. There are correlations for either free or forced convection based on dimensionless numbers. Details are described in heat transfer texts.

2.2. Condensing heat transfer

In this process, heat is removed in such a way that vapor is converted into liquid. Vapor diffuses through the vapor-air boundary layer and condenses on the liquid film. For condensation of a pure vapor, this mode is controlled by the thermal resistance of the liquid film and is proportional to the saturation to wall temperature difference $(T_{sat} - T_w)$. For atmosphere containing noncondensable gas, such as air, the major resistance to mass and heat trnasfer is the vapor-air boundary layer. The presence of noncondensable gas condiderably reduces the heat transfer coefficient relative to the vaule obtained with pure condensable vapor.

Considerable effort has been spent in studying the fundamental modes of heat transfer in condensing vapor systems. The literature is generally separated according to the description of the resultant condensate: dropwise or filmwise. *Dropwise condensation* occurs when vapor comes in contact with a non-wetting surface that is at a temperature lower than the saturation temperature of the vapor. The condensate on the non-wetting surfaces will collect in growing droplets until they run off the surface due to gravity or other external forces. Very high heat transfer rates have been reported for this type of condensation. The mechanism of the formation of the liquid drops of dropwise condensation is unclear. Generally, theories are categorized in two areas.[1] One theory hypothesize that a very thin film condenses on a surface between visible drops: the film subsequently grows to a critical thickness, and finally, the film fractures to produce droplets. The second theory suggests that the condensation begins as a consequence of a nucleation phenomena. If the condensate tends to wet the surface and thereby forms a liquid film, the process is called *filmwise condensation*. Filmwise condensation is more common and characterized by lower heat transfer rates than those of dropwise condensation. Heat transfer rates in laminar film condensation on vertical or near vertical surfaces originally predicted by Nusselt and its modification taking into account the effects of interfacial shear, fluid acceleration, nonlinear temperature distributions, and surface instabilities are made by others.

The real importance of the dropwise condensation mode of heat transfer is in the possible thermal loadings on localized structures due to the extraordinary heat flux. The dropwise condensation on the pressure response is minimal because this means of condensation is difficult to achieve because of the surface conditions required and probably is not typical for extended periods of the condensation following a LOCA. Even if extensive dropwise condensation did exist immediately after the rupture of the primary coolant system, the duration would likely be short because of the probable buildup of a water film on the containment walls and other equipments.

2.3. Variable dependence

The heat transfer process to the containment is dependent on many variables. The following ones should be mentioned[2]:

(1) Heat transfer mode (single phase convection, condensation or both).

(2) Condensation mode (filmwise or dropwise).

(3) Surface condition of heat sinks.

(4) Time after accident.

(5) Geometry and location of heat sinks.

(6) Thermal properties of heat sinks.

(7) Temperature of heat sinks.

(8) Temperature of atmosphere.

(9) Steam concentration and distribution (noncondensable gas).

(10) Steam velocity (turbulence of the atmosphere).

It is impractical to take all these factors into consideration for the heat transfer calculation. Factor (2), (3), and (10) are very difficult to model and Factor (10), although difficult to determine, is very important in the calculation of the heat transfer coefficient.[3] As a consequence of factors (1), (2), (8) and (9), the atmosphere can be saturated or superheated, which is a very important consideration for containment pressure and temperature calculations.

3. Experimental Values

Experimental values of containment heat transfer coefficient were obtained by Alf Kolflat, Uchida, CVTR tests, and Marvikken. Among these, Uchida experiments and CVTR tests are most reliable, which are described here in detail.

3.1. Uchida experimental values[2,11,12]

Uchida's experimental value is based on a series of experiments where various mixtures of steam and noncondensable gases are cooled on a vertical surface 14cm×30cm. The Uchida experiments have values of the heat transfer coefficients as a function of the air/steam weight ratio.

The heat transfer coefficient was found to be decreasing with the increase of noncondensables in the mixtures, and the coefficient is independent of the kind of noncondensables. This simple dependence makes the correlation easy to use but it also restricts its application to conditions which is nearly saturated atmospheric temperature and a low atmospheric turbulence.

Table 1. Uchica Condensing Steam Heat Transfer Coefficient

Mass Ratio (air/steam)	Heat Tansfer Coefficient (Btu/hr-ft²-°F)
≥50	2
20	8
18	9
14	10
10	14
7.0	17
5.0	21
4.0	24
3.0	29
2.3	37
1.8	46
1.3	63
0.8	98
0.5	140
≤0.1	280

3.2. CVTR tests[2]

Only limited experimental data exist for the analysis of the containment response to postulated accident conditions. The Carolinas Virginia Tube Reactor (CVTR) simulated design basis accident (DBA) tests provides the only large-scale containment (free volume of 227000ft³) response data available for evaluating computational techniques used in the safety analysis of power reactors. Time-dependent heat transfer data at various locations throughout the containment structure were obtained to assess currently accepted heat transfer correlations used in containment response computations and to provide a basis for recommendations to improve heat transfer models.

The heat transfer process, as mentioned at previous section, is dependent on many variables. Generally a detailed space-time solution for localized heat transfer coefficients is unachievable. A practice in containment response calculations for the safety analysis of power reactors

is to use area-averaged heat transfer coefficients. The average coefficient permits estimation of total structural heat absorption and, consequently, average containment pressure-temperature transient. However, the localized response may significantly differ from the average behavior. The possibility of local conditions exceeding design stress limits, pressures, or temperatures is of particular concern near the blowdown source.

The principal measurements used to determine the heat transfer behavior in the CVTR containment are as follows:

(1) Containment wall interior temperature res ponse (heat transfer assemblies).

(2) Steel liner surface-bulk atmosphere temperature differences.

(3) Other heat sink surface temperatures.

(4) Condensation rates.

(5) Heat fluxes.

(6) Energy addition versus pressure and temperature response (energy balance).

(7) Convective currents.

(8) Pressure reduction spray efficiency and spray effectiveness (temperature and pressure response measurements).

(9) Steam migration times and steam distribution (high speed photography).

Several methods of estimating containment heat transfer available in the CVTR tests are described here.

(*I*) Two heat transfer assemblies in two different locations, which measured the temperature profile through the wall as a function of time, were used to estimate the heat transfer through the containment. The measured temperature data was analyzed using an inverse heat conduction code TAEH, which calculated the unknown heat transfer coefficient from the measured temperature profile.

(*II*) As a crude method, the heat transfer coefficients were estimated from a simple energy balance in the steel liner by measuring the wall temperature and the bulk temperature as a function of time. The heat balance expression for heat transfer is as follow:

$$h(t)=\frac{\rho C_p\cdot \Delta x\cdot (dT_s/dt)}{T_\infty - T_s} \tag{1}$$

where Δx is the steel liner thickness (0.25 in.) and subscript s is referred to liner surface. Equation (1) is based on the assumption of a large liner thermal conductivity (liner surface and interior points not greatly different). The results of these estimate show the region dependence of heat transfer. The heat transfer coefficients for the basement region were observed to be much smaller than those for the upper intermediate and operating regions.

(*III*) A third method of estimating heat transfer consists of the collection of condensate from an area of about 31ft^2 and measurement of the rate of condensation. A rate of heat transfer and a heat transfer coefficient were found by assuming that the condensate gave up its latent heat of vaporization to the condensate area.

With film condensation of vapor on tall vertical surfaces, condensation rates may easily be sufficiently large to cause turbulent flow in the film. Turbulent flow has been found to commence at a critical value of the Reynolds number for the film. The critical value is found to be about 1800 for vertical surfaces when the Reynolds number defined as follows:

$$\mathrm{Re}=\frac{4W}{\mu} \tag{2}$$

where W is the mass flow rate of condensate from the lowest point on condensing surface divided by the width. For Re$<$1800, the Nusselt expression for the heat transfer coefficient h_{Nu} is:

$$h_{Nu}=1.47(\mathrm{Re})^{-1/3}\left(\frac{\mu^2}{k^3\rho^2 g}\right)^{-1/3} \tag{3}$$

where h_{Nu} is Nusselt zero vapor velocity heat transfer coefficient (Mean value of h with respect to height of condensing surface). In practice,

h is found to be larger than that of Nusselt. For low vapor velocities and Re$\leq$1800, McAdams recommends multiplication of h_{Nu} by 1.28. The effect of vapor velocities on film condensation behavior is clearly dependent on whether vapor flow is up or down the wall, and local behavior is difficult to specify from the limited velocity measurements at CVTR. In this method, an accurate time correlation between the condensation rate data and the actual test time was not obtained.

(*IV*) The fourth method was a direct measurement of the heat flux through the wall using heat flux gages. The data from the heat flux gage measurements may be low because of improper installation.

(*V*) The fifth method of obtaining energy absorption rates and average film coefficients used a computer code called RECACO, which did an energy balance between the steam energy added and the recorded temperature and pressure variations in the containment.

Table 2. Summary of Heat Transfer Coefficient Obtained in CVTR Tests

Method	Range of h (Btu/hr-ft²-°F)
I (Use TAEH Code)	20~260
II (Rough estimate using energy balance on steel lining)	5~280
IV (Use heat flux gage)	6~ 55
V (Total energy balance)	50~500

The coefficients obtained by these different methods are summarized in Table 2. The coefficienst derived by RECACO, are higher by a factor of two or three than the TAEH values, which are considered the most reliable results by the authors of the CVTR report. The coefficients obtained by method I are much larger than Uchida's experimental values, which represent the existence of some phenomena present in a large containment which were not observed in the small scale experiments. Two of these phenomena were observed in the CVTR tests: bulk velocities as high as 30ft/sec were detected inside the containment building during the test and a non-uniform temperature distribution in the containment atmosphere was observed although the total pressure was fairly uniform.

4. Empirical Correlations

4.1. Jubb's correlation[5]

In Jubb's experiments, the steam was injected into a Lancashire boiler to simulate a steam leakage into a reactor containment vessel and to enable the resultant pressure to be estimated (allowing for heat loss to the vessel). Two correlations for forced and free convectiion derived from the experimental data:

$$St \cdot Pr^{1/2} = \frac{0.0576}{(\mathrm{Re}\,P)^{1/4}}, \text{ for forced convection} \quad (4)$$

and

$$\frac{q''}{\rho} = 0.0152 \Delta T^{5/4}, \text{ for free convection} \quad (5)$$

where ΔT is the temperature difference between steam/air mixture and estimated temperature of inner wall of boiler shell. Above results were obtained over the following ranges of values:

steam flow	40-160 lb/ft²-sec
total pressure	1-8.5 atmospheres
ΔT steam-shell	35-102 °F
Re	$13\text{-}68 \times 10^6$
steam/air ratio	0-3.1

The probable errors, calculated from all points, were $+6.9\%-6.3\%$ for using Eq. (4) and $+23\%-18\%$ for using Eq. (5). The experiments were performed inside a small boiler and limited conditions, so do not seem to be applicable to large containment building.

4.2. Tagami's correlations[1,11]

The Tagami correlation is based on the

transient heat transfer data of a 15cm(diameter) by 45cm(height) vertical cylinder intide a steam-agitated container, which have been widely used in computer codes. This correlation can be expressed as follows: for the maximum heat transtfer coefficient

$$h_{max}=C\left(\frac{Q}{Vt_p}\right)^{0.62} \tag{6}$$

where C=0.603 for SIunits

C=72.5 for English units

and for the heat transfer coefficient as a function of time

$$h_{total}=h_{max}\left(\frac{t}{t_p}\right) \tag{7}$$

The correlation represents a linear time interpolation between an initial value of zero and an h_{max} which occurs at $t=t_p$. For times beyond t_p the Tagami correlation is not used. Customarily some type of a transition to the Uchida correlation is provided.

5. Analytical Models

5.1. The model of Whiley, Chan and Okrent[4]

The heat transfer process during the accident is initially characterized by a short duration of dropwise condensation and then dominated by filmwise condensation on the relatively cold surfaces. Based on the Nusselt condensation theory and the Couette boundary layer flow model, a numerical algorithm was developed to predict the heat transfer coefficient to the containment structure in terms of the prominent parameters in the containment. For engineering application, an approximated closed-form solution was also obtained as follows:

$$h=0.037\rho_\infty U_\infty i_{fg} Re^{-0.2} Sc^{-0.4}\cdot \ln\left(\frac{1-\zeta_\infty}{1-\zeta_w}\right)\cdot\frac{1}{(T_\infty-T_{ic})} \tag{8-1}$$

or

$$h=0.037\rho_\infty i_{fg}\nu_\infty^{0.2} U_\infty^{0.8} L^{-0.2} Sc^{-0.4}\cdot \ln\left(\frac{1-\zeta_\infty}{1-\zeta_W}\right)\cdot\frac{1}{(T_\infty-T_W)} \tag{8-2}$$

The restriction of Eq. (8) is that the interfacial temperature between the liquid and the vapor phase to the wall temperature and the sensible heat is small in comparison with the latent heat.

This model predicts that the heat transfer coefficient increases with increasing velocity, lower driving temperature, lower air/steam ratio and decreasing film length. They obtained higher values for the heat heat transfer coefficient than the values obtained using the Uchida or the Tagami correlations.

5.2. The model of Braddy, Schoenhoff and Thiesing[6]

This model used in Pechtel containment code, COPATTA, which calculates the total heat removal from

$$\dot{q}=h_{cond}A(T_{sat}-T_W)+\dot{q}_{conv} \tag{9}$$

where $\dot{q}_{conv}$ is the free-convection heat transfer term. This model also removes mass and superheats the containment atmosphere.

5.3. The model of Krotiuk and Rubin[7]

In this model, the convection and condensation terms were solved for separately assuming the followings:

(1) A laminar condensing liquid film exists on the heat sink surface, which possesses no surface-dependent temperature gradient.

(2) The temperature gradient in the condensation film is small compared to gradient in the gaseous boundary layer from the containment gaseous region far from the heat sink surface to the condensing film gaseous-liquide interface. Therefore, the vapor-liquid interace temperature is assumed equal to the wall temperature.

(3) Thermodynamic properties are assumed to be constant values within the gaseous boundary layer and can be calculated at the gaseous film reference temperature.

(4) The containment atmosphere is assumed

to possess homogeneous temperature, pressure, and composition except at heat sink surfaces.

(5) The steam partial pressure at the vapor-liquid interface is equal to the saturation pressure at the temperature of the vapor-liquid interface.

Under the above assumptions, condensing heat and mass transfer using diffusion methods were solved for directly.

$$\dot{q}_{total}=\dot{q}_{conv}+\dot{q}_{cond} \tag{10}$$

$$\dot{q}_{conv}=h_{conv}A(T_{vapor}-T_w) \tag{11}$$

$$\dot{q}_{cond}=\dot{m}_{cond}(i_{gsat}-i_{fw}) \tag{12}$$

where the averge value of the h_{conv} is calculated using the appropriate Nusselt number correlation for either turbulent forced convection or free convection. The value of the steam mass condensation rate is calcuted from the mass diffusion correlation:

$$\dot{m}_{cond}=G_gM_gA\frac{(X_{\infty g}-X_{ig})}{(X_{ia}-X_{\infty a})/\ln(X_{ia}/X_{\infty a})} \tag{13}$$

The condensing heat transfer coefficeient is calculated when condensation dominates (only free convection) as:

$$h_{cond}=\frac{\dot{q}_{total}}{A(T_{sat}-T_w)} \tag{14}$$

or when forced convection exists

$$h_{cond}=\frac{\dot{q}_{total}}{A(T_{vapor}-T_w)} \tag{15}$$

Although the obtained value for h_{cond} agree reasonably well with the experimental CVTR 3 values, the calulated pressure and temperature using this model in the computer code CONTEMPT-LT are much higher than the measured values.

5.4. The model of Mansfield[3]

Mansfield uses the Tagami correlation in the program COFLOW as follows:

before the end of the blowdown (British units)

$$h_{total}=h_{max}\left(\frac{t}{t_p}\right)^{0.5} \tag{16}$$

where h_{max} is same in Eq. (6)

After the blowdown ends

$$h_{total}=h_{stag}+(h_{max}-h_{stag})e^{-0.05(t-t_p)} \tag{17}$$

where

$$h_{stag}=2+50x \tag{18}$$

5.5. The model of Frank, Hynek and Stauder[8]

This model is useful in determining the PWR containment response to a postulated main steam line break (MSLB) during the period prior to spray initiation, when the containment atmosphere is superheated.

$$\dot{q}_{cond}=h_{cond}A(T_{sat}-T_w) \tag{19}$$

$$\dot{q}_{conv}=h_{conv}A(T_\infty-T_{sat}) \tag{20}$$

and the mass transfer rate from the atmosphere

$$\dot{m}=\frac{\dot{q}_{cond}-\dot{q}_{conv}}{i_g(T_\infty)-i_f(T_{sat})} \tag{21}$$

For h_{cond}, the Uchida correlation is used. For h_{conv}, a value of 114w/m²-k (20Btu/hr-ft²-°F) fits the highest measured containment atmosphere temperature transient from CVTR test 3.

5.6. The model of Lamkin and Gido[9]

Considering a bounday layer above the condensate, the energy transfer to the heat sinks is evaluated based on mass and energy balances on the control volume abcd (Fig. 2).

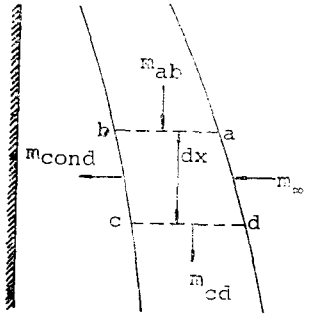

Fig. 2. Sketch of Control Volume.

$$\dot{q}_{total}=\dot{m}_{\infty a}(i_{\infty a}-i_a)+(\dot{m}_{\infty g}-\dot{m}_{cond})(i_{\infty g}-i_g)+\dot{m}_{cond}(i_{\infty g}-i_f) \tag{22}$$

with a value of $\dot{m}_{\infty g}/\dot{m}_{cond}\geq 1$. The first term on the right hand side of Eq. (22) accounts for the heat transferred by air to the boundary

layer between the condensate film and the containment atmosphere. The second term accounts for the heat transferred by steam to this boundary layer and finally the last term acconts for the heat transferred by the condensate.

5.7. The model of Corradini[10]

In this model, a turbulent condensation model is derived for natural and forced convection considering noncondensable gases using the Reynolds-Colburn turbulent analogy for mass and momentum transfer. The Reynolds-Colburn analogy states that heat transfer coefficent (Stanton No.) is proportional to the wall friction factor and to the ratio of turbulent heat transport to momentum transport. Corradini apply this analogy to the mass transfer coefficient, G, and derived the equations:

for forcced convection

$$h_{conv}=0.037\frac{k_a}{L}\mathrm{Re}^{0.8}\mathrm{Pr}^{1/3} \tag{23}$$

for natural convection

$$h_{conv}=0.0246\frac{k_a}{L}\mathrm{Gr}^{2/5}\mathrm{Pr}^{7/15}(1+0.5\mathrm{Pr}^{2/3})^{-2/5} \tag{24}$$

for condensation heat transfer coefficient

$$h_{cond}=\frac{q''}{(T_\infty-T_w)} \tag{25}$$

$$h_{cond}=\left(\frac{1}{h_{film}}+\frac{1}{h_{gas}}\right)^{-1}\cong h_{gas} \tag{26}$$

$$h_{gas}=\frac{\dot{m}''[i(T_\infty)-i(T_i)]}{T_\infty-T_i}+h_{conv} \tag{27}$$

$$\dot{m}''=G(X_\infty-X_i) \tag{28}$$

This mdoel is applicable to the mass transfer of steam and convective heat transfer through the gas/vapor boundary layer. Normally, with noncondensables present, the resistance of liquid film is small compared to the gas/vapor boundary layer resistance. For an assumed velocity of 2m/s, the good agreement with the Tagami data is obtained.

5.8. The model of Almenas[11]

In this model, the mass, energy and momentum balance equations are solved in an air-vapor boundary layer adjoining a vertical condensing surface. The resultant expressions are as follows:

$$q''_{total}=Aq''_{cond}+ABq''_{conv} \tag{29}$$

$$q''_{cond}=\rho_i i_{fg} d\left(\frac{\rho_\infty}{\rho_i}-\frac{\rho_{\infty a}}{\rho_{ia}}\right) \tag{30}$$

$$q''_{conv}=5d\left(\frac{\rho_{\infty a}}{\rho_{ia}}\right)\overline{(C_p\rho)}\,(T_\infty-\bar{T}) \tag{31}$$

where

$$d=0.46D^{1/2}\left[\frac{\bar{\rho}}{g\Delta\rho}\left(\mathrm{Sc}+1.14\frac{\rho_{\infty a}}{\rho_{ia}}\right)\frac{\rho_{\infty a}}{\rho_{ia}}\right]^{-1/4}L^{-1/4} \tag{32}$$

These expressions yield the total heat transfer rate rather than the more customary heat transfer coefficient. This model was intended to calculate heat transfer from saturated and superheated atmospheres, which results from MSLB.

6. Discussion

(1) Although it may be conservative to have a higher containment pressure (i.e., underpredicted heat transfer coefficient) for structural evaluation of containment, but it is less conservative for analyzing the ECCS.[4] In accordance with 10 CFR Part 50, Appendix A "General Design Criteria for Nuclear Power Plants", Section V: Reactor containment, Criteria 50-Containment design basis: The reactor containment structure, including access openings, penetrations, and the containment heat removal system shall be designed so that the containment structure and its internal compartments can accomdate, without exceeding the design leakage rate and, with sufficient margin, the calculated pressure and temperature conditions resultings from any LOCA. On the other hand, Appendix K states that the containment pressure used for evaluating cooling effectiveness during reflood and spray cooling shall not exceed a pressure calculated conservatively for this purpose.

In reactor licensing, two different sets of heat transfer coefficients are used depending whether the calculated containment pressure is used for containment design or for the evaluation of the ECCS. For the former case, the following heat transfer coeffiicent h is being used in may license applications:

a) During the blowdown phase, h is a linear increasing function from an initial value of zero to a peak value h_{max} at the end of blowdown where h_{max} is given by the Tagami correlation.

b) After the peak, h is given by the Uchida correlation.

In the evaluation of the back pressure for ECCS, the following heat transfer coeffiicients are used,

a) During the blowdown phase, h increases linearly from an initial value of 8 Btu/hr-ft^2-F to a peak value four times greater than the maximum calculated from the Tagami correlation at the end of blowdown.

b) During the long term stagnation phase of the accident, characterized by low turbulence in the containment atmosphere, the condensing heat transfer coefficient h_{stag} is 1.2 times greater than that predicted by the Uchida data.

c) For the transition phase of the accident between the end of blowdown and the long term post-blowdown phase, an exponential transion in the condensing heat transfer coefficient is assumed as

$$h=h_{stag}+(h_{max}-h_{stag})e^{-0.025(t-t_p)} \quad (33)$$

(2) The Tagami and Uchida correlations seem to be scale dependent[3]. A multiplier of four or five was needed to obtain agreement for the calculated peak pressure and peak temperature of the CVTR experiments, using the program CONTEMPT-LT. It can be questioned if a larger multiplier than four or five will be needed to obtain best estimate results for commercial power plant containments because the CVTR containment is smaller than the commercial PWR containment.

(3) Although the dominent condensation mode on the wall of containment building is filmwise condensation, local dropwise condensation could occur especially in early portion of blowdown phase[1]. The extraordinary heat flux of dropwise condensation can cause serious thermal loadings on the affected structures.

(4) Heat transfer coefficient is dependent on many variables such as condensation mode, steam concentration and distribution, thermal resistance of the condensate film, surface conditions, concentration of impurities and noncondensables, time after accident and steam turbuelnce[2]. Heat transfer coefficient is very small in initially but increase to the peak value rapidly by turbulence mixing during the blowdown, as the blowdown ceases, then decreases rapidly to significant low.

(5) Painted surface may tend to promote dropwise condensation that would greatly enhance the heat transfer during the early portion of blowdown and result in a lower peak pressure[1]. On the other hand, for filmwise condensation, the presence of paint would cause an added resistance and would tend to impede the heat transfer.

Nomenclature

A	area of heat sink
A, B	empirical normalizatcn ccnstants for Eq. (29)
C_p	specific heat capacity at constant pressure
g	accelation of gravity
G	mass transfer coefficient
h	heat transfer coefficient
i	specific enthalpy
k	thermal conductivity
L	perimeter cr height of condensing surface
M	molecular weight
$\dot{m}$	mass rate
$\dot{m}''$	mass flux of steam condensing on cold surface
P	Pressure

Pr	Prandtl number
Q	totoa energy released
q''	heat flux
$\dot{q}$	heat transfer rate
Re	Reynolds number
Sc	Schmidt number
St	Stanton number
T	temperature
t	time
U	velocity of vapor
v	containment volume
x	steam/air mass ratio
ρ	density
μ	viscosity
ζ	mass fraction of air

Subscripts

a	air in the boundary layer
cond	condensation
conv	convective
f	liquid film
g	vapor
i	interface
max	maximum
Nu	Nusselt condensing (pure steam)
p	peak
sat	saturation
$stag$	stagnation
w	wall
∞	atmosphere
∞a	air through air-vapor boundary layer
∞g	steam through air-vapor boundary layer

References

1. D.C. Slaughterbeck, Review of Heat Transfer Coefficients for Condensing Steam in a Containment Building Following a LCCA, IN-1388 (1970).
2. R.C. Schmitt, G.E. Bingham, and J.A. Norberg, Simulated Design Basis Accident Tests of the Carolinas Virginia Tube Reactor containment, IN-1403 (1970).
3. J.J. Carbajo, Heat Transfer Coefficients under LOCA conditions in Containment Building, Nucl. Eng. & Design, 65, 369(1981).
4. R.H. Whitley, C.K. Chan, and D. Okrent, On the Analysis of Containment Heat Transfer Following a LOCA, Ann. Nucl. Eng. 3(1976).
5. D.H. Jubb, Condensation in a Reactor Containment Vessel, Nucl. Eng., 431(1959).
6. R.G. Braddy, H.M. Schoenhoff, and J.W. Thiesing, Surface Temperature Response of Equipment inside Containment Following Pipe Break, Trans. Am. Nucl. Soc., 24, 319(1976).
7. W.J. Krotiuk and M.B. Rubin, Condensing Heat Transfer Following a LOCA, Nucl. Tech., 37, 118(1978).
8. S. Frank, S.J. Hynek, and J.W. Stauder, Superheated Containment Atmosphere Heat/Mass Transfer to Passive Heat Sinks, Trans. Am. Nucl. Soc., 28, 408(1978).
9. D.E. Lamkin and R.G. Gido, A New Condensation Mass Removal Model for Containment Analysis, Trans. Am. Nucl. Soc., 30, 372(1978).
10. M.L. Corradini, Condensation on a Wall in the Presence of Noncongensable Gas, Trans. Am. Nucl. Soc., 43, 484(1982).
11. K. Almenas, Heat Transfer from Saturated and Superheated Atmospheres for Containment Analysis, Nucl. Eng. Design, 71, 1(1982).
12. D.W. Hargroves et al., CONTEMPT-LT/028-A Computer Program for Predicting Containment Pressure-Temperature Response to a LOCA, NUREG/CR-0255 (1979).
13. P.S. Ayyaswany, J.N. Chung, and K.K. Niyogi, Reactor Containment Heat Removal by Passive Heat Sinks Following a LCCA, Trans. Am. Nucl. Soc., 23, 305(1976).
14. G. Poots and R.G. Miles, Effects of Variable Physical Properties on Laminar Film Condensation of Saturated Steam on a Vertical Flat Plate, Int. J. Heat Mass Transfer, 10, 1677 (1967).
15. D.C. Slaughterbeck, Pressure Responses of PWR Containments-A Parametric Analysis, IDO-17300 (1969).
16. J.M. Marchello and K.K. Almenas, The Physical State of Post LOCA Containment Atmospheres, Nucl. Tech., 44, 411(1979).

17. W.J. Minkowycz bnd E.M. Sparrow, Condensation Heat Transfer in the Presence of Noncondensables, Interfacial Resistance, Superheating, Variable Properties, and Diffusion, Int. J. Heat Mass Transfer, 9, 1125(1966).

18. S.H. Chang, Theoretical and User's Manual of COPATTA-10; Containment Pressure and Temperature Transient Analysis Code 1982, Bechtel Power Corporation.